

# Separable form of low-momentum realistic NN interaction

P. Grygorov,<sup>1</sup> E.N.E. van Dalen,<sup>1</sup> J. Margueron,<sup>2</sup> and H. Mütter<sup>1</sup>

<sup>1</sup>*Institut für Theoretische Physik, Universität Tübingen, D-72076 Tübingen, Germany*

<sup>2</sup>*Institut de Physique Nucléaire, Université Paris-Sud, F-91406 Orsay CEDEX, France*

The low-momentum interaction  $V_{\text{low-k}}$  derived from realistic models of the nucleon-nucleon interaction is presented in a separable form. This separable force is supported by a contact interaction in order to achieve the saturation properties of symmetric nuclear matter. Bulk properties of nuclear matter and finite nuclei are investigated for the separable form of  $V_{\text{low-k}}$  and two different parameterizations of the contact term. The accuracy of the separable force in Hartree-Fock calculations with respect to the original interaction  $V_{\text{low-k}}$  is discussed. For a cutoff parameter  $\Lambda$  of  $2 \text{ fm}^{-1}$  a representation by a rank 2 separable force yields a sufficient accuracy, while higher ranks are required for larger cut-off parameters. The resulting separable force is parameterized in a simple way to allow for an easy application in other nuclear structure calculations.

PACS numbers: 21.60.Jz, 21.65.+f, 26.60.+c, 97.60.Jd

Keywords: Nuclear matter, finite nuclei, neutron star crust.

## I. INTRODUCTION

The evaluation of bulk properties of finite nuclei and nuclear matter starting from realistic models of nucleon-nucleon (NN) interaction is a major challenge in modern nuclear physics. Since the exact form of the interaction resulted from the underlying theory of the strong interaction remains unknown, one usually has deal with realistic models developed so as to fit experimental data for free nucleon-nucleon scattering up to the threshold for pion production and properties of the deuteron [1]-[4]. It was done by obtaining a best fit for a large number of adjustable parameters using several thousands experimental points so that there exists several quite different potential models commonly used. A general feature of such realistic interactions is strong short-range and tensor components, which cannot be handled within the standard perturbation theory. There have been suggested different approaches in order to overcome this problem: Bethe-Brueckner-Goldstone expansion [5], correlated basis functions [6], quantum Monte Carlo [7], self-consistent Green's function theory (see, e.g., Ref. [8]). These methods were successfully applied to describe bulk properties of nuclear matter [9], pairing gap of nucleons [10], weak response [11] and shear viscosity of nuclear matter [12]. However these approaches remain very complex to be applied directly to a description of finite nuclei, as well as inhomogeneous nuclear matter, also known as pasta phase, which exists in the inner crust of neutron stars. Alternatively, they have been combined either to phenomenological approaches through a local density approximation [13], or as an input for a density functional approach [14]. In these approaches, adjustable parameters need however to be determined.

Besides the realistic interactions, various phenomenological models have been developed, such as the Skyrme interaction [15], and adjusted to describe the experimental data for the ground states of finite nuclei and the empirical saturation point of symmetric nuclear matter. A simple parameterization of such phenomenological forces through the local single-particle densities allows a simple solution of the Hartree-Fock (HF) equations [16]. Finally, these models have been successfully used for predictions of equations of state (EoS) of nuclear matter and description of pasta phase within the Wigner-Seitz (WS) cell approximation [17]. In neutron stars, these models are extrapolated far from the condition where it has been adjusted and might in some cases become unstable [18]. The instabilities of these models could however be corrected such as it reproduces the features of a G-matrix in nuclear matter [19].

An alternative method, which is based on realistic NN interactions and allows us to perform Hartree-Fock calculations similarly to the phenomenological forces is the low-momentum interaction  $V_{\text{low-k}}$ . The basic idea of  $V_{\text{low-k}}$  is to separate the predictions for correlations at low momenta, which are constrained by the NN scattering matrix below the pion threshold, from the high-momentum components, which may strongly depend on the underlying model of realistic NN interaction. By introducing a cutoff  $\Lambda$  in momentum space, one separates the Hilbert space into a low-momentum and a high-momentum part. The renormalization technique (see, e.g., [20–24]) determines an effective Hamiltonian, which must be diagonalized within the model space (below the cutoff). With the cutoff in the range of  $\Lambda = 2 \text{ fm}^{-1}$   $V_{\text{low-k}}$  becomes model independent, and reproduces the deuteron binding energy, low-energy phase shifts, and half-on-shell  $T$  matrix with the same accuracy as the initial realistic interaction. This model independence demonstrates that the low-momentum physics does not depend on details of the high-momentum dynamics.

In spite of its obvious advantages  $V_{\text{low-k}}$  potential still remains a quite complicated object. On the one hand, it is nonlocal and therefore is represented as a matrix element in momentum space for each partial wave channel. This nonlocality increases the computational time in Hartree-Fock iterations, and prevents the use of  $V_{\text{low-k}}$  if the number

of nucleons is too large, such as in the Wigner-Seitz cells present in the crust of neutron stars for instance [17]. On the other hand, the renormalization technique used to produce  $V_{\text{low-k}}$  seems not to be trivial. The resulting interaction is given as a matrix table which is not an easy-to-use form and prevents this potential to be popular. A possible way out is to find a separable representation of  $V_{\text{low-k}}$ , since it significantly simplifies many-body calculation [25, 26]. Moreover recent calculations of triton binding energies demonstrate the  $V_{\text{low-k}}$  can be very good approximated by a low-rank separable force for low values of the cutoff  $\Lambda$  [27]. We investigate the separability of  $V_{\text{low-k}}$  by using the diagonalization of the matrix in momentum space for each partial wave channel. It allows us to find a low rank separable form of  $V_{\text{low-k}}$ , which can be used in HF calculations of nuclear matter as well as finite nuclei.

The  $V_{\text{low-k}}$  Hartree-Fock calculations demonstrate a monotonic increase of the binding energy of symmetric nuclear matter as a function of the nucleon density, thus it cannot reproduce the empirical saturation point [28, 30]. Therefore we supplement  $V_{\text{low-k}}$  by a simple density-dependent contact term, which accounts for a three-body correlations. This contact term is adjusted to reproduce the saturation property of symmetric matter.

The paper is organized as follows. In the next Section II we discuss the model space technique used to produce  $V_{\text{low-k}}$  and outline the procedure to determine the separable representation. In the last Section III we sum up all results and suggest a simple fit for separable representation of  $V_{\text{low-k}}$  as well as two different parameterizations of the contact term, adjusted for the fitted potential.

## II. MODEL OF THE NN INTERACTION

The main idea of  $V_{\text{low-k}}$  interaction is to disentangle the low-momentum or long-range part of a realistic NN interaction, which is fairly well described in terms of meson-exchange, from the high-momentum or short-range part where quark degrees of freedom are getting important. In other words, one defines a model space, which accounts for the low-momentum degrees of freedom and renormalizes the effective Hamiltonian for this low-momentum regime in order to account for the effects of the high-momentum components, which are integrated out.

In practice the  $V_{\text{low-k}}$  interaction can be derived either using model space methods (such as Lee-Suzuki [21] or Okubo [22]) or through an renormalization group treatment [20]. Both approaches are essentially equivalent and lead to the same energy-independent potential [23]. In the following we will use the model space technique to disentangle these parts based on the unitary model operator approach (UMOA). This approach has frequently been described in the literature [24, 28, 29]. Therefore we will restrict the presentation only to basic equations, which will define the nomenclature.

To determine the model space, the low-momentum subspace of Hilbert space, one defines a projection operator  $\hat{P}$ , which projects onto this model space. The complement of the subspace will be defined by the projection operator  $\hat{Q}$ , in such a way that the whole space is covered by these two operators. Thus they satisfy the following relations  $\hat{P} + \hat{Q} = 1$ ,  $\hat{P}^2 = \hat{P}$ ,  $\hat{Q}^2 = \hat{Q}$ ,  $\hat{P}\hat{Q} = 0 = \hat{Q}\hat{P}$ . The unitary model operator approach defines a unitary transformation  $\hat{U}$  in such a way that the transformed Hamiltonian does not couple the  $\hat{P}$  and  $\hat{Q}$  space, i.e.,

$$\hat{Q}\hat{U}^{-1}\hat{H}\hat{U}\hat{P} = 0. \quad (1)$$

Now the effective two-body interaction of Hermitian type can be determined in terms of unitary transformation  $\hat{U}$  as

$$V_{\text{eff}} = V_{\text{low-k}} = \hat{U}^{-1}(\hat{h}_0 - \hat{v}_{12})\hat{U} - \hat{h}_0, \quad (2)$$

where  $\hat{v}_{12}$  stands for the bare NN interaction. The operator  $\hat{h}_0$  denotes the one-body part of the two-body system and contains the kinetic energy of the interacting particles. It is important to notice that in any case  $\hat{h}_0$  commutes with the projection operators  $\hat{P}$  and  $\hat{Q}$ . As it was shown by Suzuki [24] the operator  $\hat{U}$  is expressed as

$$\hat{U} = (1 + \hat{\omega} - \hat{\omega}^\dagger)(1 + \hat{\omega}\hat{\omega}^\dagger + \hat{\omega}^\dagger\hat{\omega})^{-1/2}, \quad (3)$$

where an operator  $\hat{\omega}$  fulfills relations  $\hat{\omega} = \hat{Q}\hat{\omega}\hat{P}$  and  $\hat{\omega}^2 = \hat{\omega}^\dagger{}^2 = 0$ . To evaluate the matrix elements of this operator  $\hat{\omega}$  one should first solve the two-body eigenvalue equation

$$(\hat{h}_0 + \hat{v}_{12})|\Phi_k\rangle = E_k|\Phi_k\rangle. \quad (4)$$

From eigenstates  $|\Phi_k\rangle$  we determine those eigenstates  $|\Phi_p\rangle$ , which have the largest overlap with the  $\hat{P}$  space. After the respective matrix elements of  $\hat{\omega}$  and later  $\hat{U}$  may be defined in terms of  $\hat{P}(\hat{Q})$  eigenstates. This matrix element of  $\hat{U}$  can then be used to determine the matrix elements of the effective interaction  $V_{\text{eff}}$  in  $\hat{P}$  space (for the details see [28, 29]). In this way, one obtains the effective Hamiltonian  $\hat{H}_{\text{eff}} = \hat{h}_0 + \hat{V}_{\text{eff}}$ . Diagonalising it in the low-momentum

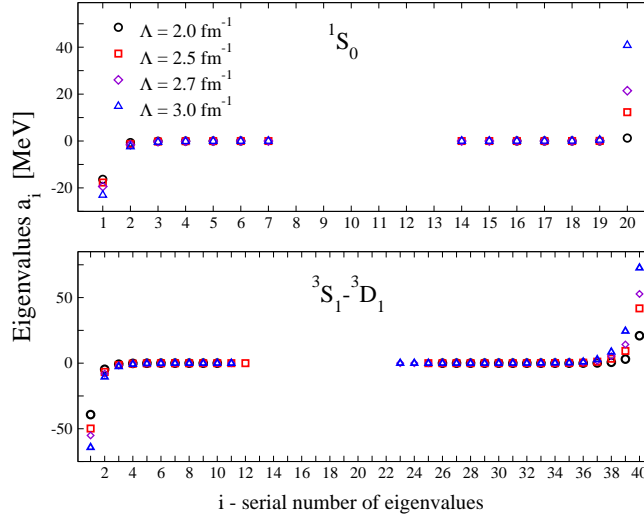


FIG. 1: (Color online) Top: Nonzero eigenvalues  $a_i$  of  $^1S_0$  channel. Bottom: Nonzero eigenvalues  $a_i$  of  $^3S_1$ - $^3D_1$  channel.

model space ( $\hat{P}$  space), one obtains eigenvalues which are identical to the diagonalization of the original Hamiltonian  $\hat{h}_0 + \hat{V}$  in the complete space. Moreover, the solution of the Lippmann-Schwinger equation for NN scattering phase shifts using  $V_{\text{low-k}}$  with a cutoff  $\Lambda$  yields the same phase shifts as obtained from original interaction  $\hat{v}_{12}$  without a cutoff. If the underlying interaction is a realistic interaction, fitted to reproduce the experimental phase shifts below  $\Lambda$ , these phase shifts will be also reproduced by  $V_{\text{low-k}}$ .

If the cutoff  $\Lambda$  is chosen around  $\Lambda = 2 \text{ fm}^{-1}$  the resulting  $V_{\text{low-k}}$  is found to be essentially model independent, i.e., is independent on the underlying realistic interaction  $\hat{v}_{12}$ . In this sense  $V_{\text{low-k}}$  is unique and, as it reproduces the NN scattering phase shifts it can also be regarded as a realistic interaction as, e.g., the CD-Bonn [1] or Argonne V18 [2] potentials.

Originally  $V_{\text{low-k}}$  is nonlocal and defined in terms of matrix elements in a basis of NN states labeled by relative momentum for pairs of nucleons. Thus for each partial wave channel there exists a matrix, which represents  $V_{\text{low-k}}(k, k')$  on a mesh of  $N$  discretized relative momenta  $k$  and  $k'$  in the range  $0 \leq k, k' \leq \Lambda$ . Since this matrix is real and symmetric with respect to  $k, k'$  one can diagonalize it, so that, it can be written as a sum of  $N$  real eigenvalues multiplied with the respective eigenvectors

$$V_{\text{low-k}}(k, k') = \sum_{i=1}^N a_i f_i^*(k) f_i(k'), \quad (5)$$

where  $N$  is the number of mesh-points and the dimension of  $V_{\text{low-k}}$  matrix. The eigenvectors  $f_i(k)$  satisfy the orthogonality relation

$$\frac{2}{\pi} \int_0^\Lambda dk k^2 f_i(k) f_j(k) = \delta_{ij}. \quad (6)$$

In the following we will omit the symbol of complex conjugation because all eigenvectors are real. The last equality (5) is nothing else but the general definition of a separable potential of the rank  $N$ . If the rank of the separable potential equals the dimension of the matrix  $V_{\text{low-k}}(k, k')$  the whole information is exactly restored from the eigenvalues  $a_i$  and eigenvectors  $f_i$ . As we will see later, some of eigenvalues  $a_i$  can be zero or negligibly small so that one can reduce the rank of separable interaction taking into account only the  $n$  eigenvalues with largest absolute values. It leads to a new approximated separable interaction  $V_{\text{low-k}}^{[n]}(k, k')$

$$V_{\text{low-k}}(k, k') \simeq V_{\text{low-k}}^{[n]}(k, k') = \sum_{i=1}^n a_i f_i(k) f_i(k'), \quad (n \leq N). \quad (7)$$

The low-rank separable representation of NN interaction leads to significant simplifications in many-body calculations.

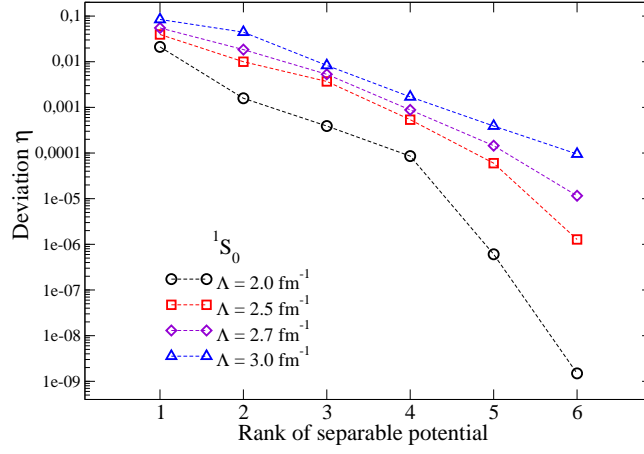


FIG. 2: (Color online) Squared deviation of the separable  $V_{\text{low-k}}^{[n]}(k, k')$  from the original  $V_{\text{low-k}}(k, k')$  in  $^1S_0$  channel for different values of the cutoff parameter  $\Lambda$ .

The effective interaction  $V_{\text{low-k}}$  as well as its separable form is nonlocal and defined in terms of matrix elements in momentum space. It implies that the HF calculations has to be performed in a Hilbert space using an appropriate basis  $|\alpha\rangle, |\beta\rangle, \dots$ . The HF Hamiltonian is then expressed in terms of the matrix elements between these basis states  $\langle\alpha|H_{\text{HF}}|\beta\rangle$  and the HF single-particle (s.-p.) states  $|\Psi_n\rangle$  are expressed through the expansion coefficients in the basis

$$|\Psi_n\rangle = \sum_{\alpha} |\alpha\rangle \langle\alpha|\Psi_n\rangle = \sum_{\alpha} c_{n\alpha} |\alpha\rangle. \quad (8)$$

The part of the HF Hamiltonian originating from  $V_{\text{low-k}}$  can be expressed in terms of two-body matrix elements by

$$\langle\alpha|H_{\text{low-k}}|\beta\rangle = \sum_{\gamma,\delta} \langle\alpha\gamma|V_{\text{low-k}}|\beta\delta\rangle \rho_{\gamma\delta}, \quad (9)$$

where  $\rho_{\gamma\delta}$  is the single-particle density matrix. In order to investigate the bulk properties of finite nuclei we perform HF calculations within the spherical Wigner-Seitz cell assuming a plane wave single-particle basis [31, 32].

### III. RESULTS AND DISCUSSION

In the following we discuss results for symmetric nuclear matter as well as finite nuclei obtained from HF calculations. These calculations are performed in the model space, which is defined by a cutoff parameter  $\Lambda$  in the two-body scattering equation, employing the corresponding low-momentum interaction  $V_{\text{low-k}}$ , which is derived from the CD-Bonn [1] interaction using the technique described in Sec.II. The NN interaction has been restricted to partial waves with total angular momentum  $J$  less equal 6.

We start our discussion with the comparison of the eigenvalues  $a_i$  obtained from diagonalization of  $20 \times 20$  matrix of  $V_{\text{low-k}}(k, k')$  in  $^1S_0$  channel. The resulted nonzero eigenvalues are shown on the top of Fig.1 for different values of  $\Lambda$ . As it was discussed above,  $V_{\text{low-k}}$  interaction becomes model independent at  $\Lambda = 2 \text{ fm}^{-1}$ . At this value of the cutoff parameter  $\Lambda$  the diagonalization procedure yields only 11 nonzero eigenvalues, other words,  $V_{\text{low-k}}$  interaction in  $^1S_0$  channel is a separable interaction of the 11th rank or, following (5), one can write

$$V_{\text{low-k}}^{[11]}(k, k') = V_{\text{low-k}}(k, k'). \quad (10)$$

The nonzero eigenvalues are essentially independent on  $N$ , the dimension of the matrix representing  $V_{\text{low-k}}$ . Going further one can notice, that many of the nonzero eigenvalues are nevertheless very small, and only some of them, e.g., at  $i = 1, 2, 20$  carry the main part of the information about the interaction model. This gives rise to a substantial lowering of the rank of separable potential, as it was shown in Eq.(7). With the increase of the cutoff  $\Lambda$  the absolute values of the eigenvalues increase as well and as a consequence the rank  $n$  of the separable form  $V_{\text{low-k}}^{[n]}$  defined in (7) has to be increased to achieve a reasonable accuracy. Increasing  $\Lambda$  more information about the short-range components

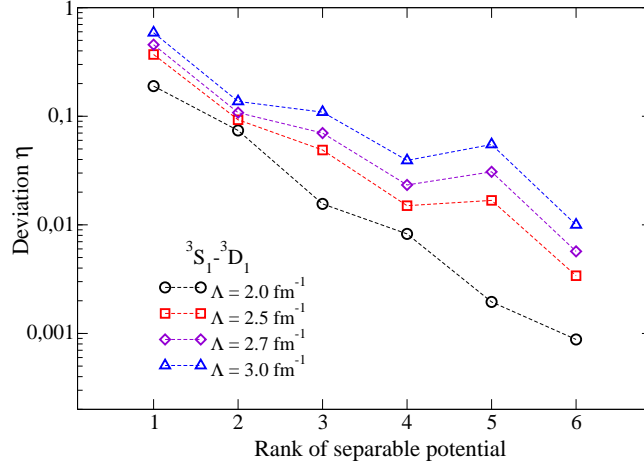


FIG. 3: (Color online) Squared deviation of the separable  $V_{\text{low-k}}^{[n]}(k, k')$  from the original  $V_{\text{low-k}}(k, k')$  in  ${}^3S_1$ - ${}^3D_1$  channel for different values of the cutoff parameter  $\Lambda$ .

of the underlying bare interaction is included, which requires a larger rank in the separable representation of the interaction.

In case of the coupled channels, like  ${}^3S_1$ - ${}^3D_1$  channel, the dimension  $N$  of the  $V_{\text{low-k}}$  matrix is twice as large if one keeps the number of mesh-points in each channel the same as for the uncoupled partial waves. It turns out that also the number of nonzero eigenvalues increases as shown in the lower panel of Fig.1. It is obvious that the rank of the separable potential should be higher than for  ${}^1S_0$  channel. It is a general feature that coupled channels require higher rank separable interaction than the uncoupled ones [33]. Also one observes pairs of positive and negative eigenvalues which have about the same absolute value. This picture remains for higher values of  $\Lambda$ . As we will see later, this symmetry between positive and negative eigenvalues will play a crucial role in the convergence of the separable form  $V_{\text{low-k}}^{[n]}$  to the initial  $V_{\text{low-k}}$  with increase of rank.

In order to determine a minimal rank for a reliable separable approximation in each channel we calculate the square deviation  $\eta$  of the separable form  $V_{\text{low-k}}^{[n]}$  from the original potential  $V_{\text{low-k}}$  for each rank  $n$

$$\eta = \sum_{k, k'} \left| V_{\text{low-k}}(k, k') - V_{\text{low-k}}^{[n]}(k, k') \right|^2 / \sum_{k, k'} |V_{\text{low-k}}(k, k')|^2. \quad (11)$$

In Fig.2 the deviation for  ${}^1S_0$  channel at different values of the cutoff  $\Lambda$  is shown. At  $\Lambda = 2 \text{ fm}^{-1}$  one observes a fast convergence to zero deviation already at the rank  $n = 2$ . The growth of the cutoff monotonically increases the rank of the separable potential. At  $\Lambda = 3 \text{ fm}^{-1}$  one may expect a good accuracy starting from  $n = 5$ .

The deviation  $\eta$  for  ${}^3S_1$ - ${}^3D_1$  channel is displayed in Fig.3. First, at low  $n$  the absolute value of the deviation is one order of magnitude higher than for uncoupled  ${}^1S_0$  channel. Increasing the rank one observes a non-monotonic, oscillating decrease of  $\eta$ , specially for high  $\Lambda$ . As we have seen, the diagonalization of the channel  ${}^3S_1$ - ${}^3D_1$  yields both positive and negative eigenvalues, which are symmetrically distributed over  $i$ . So that they form "pairs" with very similar absolute values. Assuming the odd rank we take into account either uncompensated positive or negative eigenvalue. This eigenvalue will be compensated in the next (even) rank, and the accuracy will be significantly improved.

The deviation  $\eta$  for various other channels at  $\Lambda = 2 \text{ fm}^{-1}$  is shown in Figs.4, 5. In the following we choose the second rank approximation for the uncoupled channels ( $n = 2$ ) and the third rank for the coupled one ( $n = 3$ ). Below, the respective separable version of  $V_{\text{low-k}}$  will be referred to as  $V_{\text{low-k}}^{[2,3]}$ .

Now let us turn to the binding energy of symmetric nuclear matter, which is displayed in Fig. 6. The HF calculations using  $V_{\text{low-k}}^{[2,3]}$  (dashed line) yields essentially the same result as the one employing the original  $V_{\text{low-k}}$  interaction (solid curve). The deviation does not exceed 1% at the saturation density  $\rho_0$  and 1.7% at the density  $2\rho_0$ . We also compared the binding energy of pure neutron matter for both potentials and found that the discrepancy is less than 1% for the same range of densities.

However, neither of the 2 calculations yields a saturation point, i.e. a minimum in the energy versus density plot, as it has been observed before [30, 34]. This absence of the saturation is one of the main problems in calculations of nuclear matter employing  $V_{\text{low-k}}$ . It cannot be cured by the inclusion of correlations beyond the HF approximation,

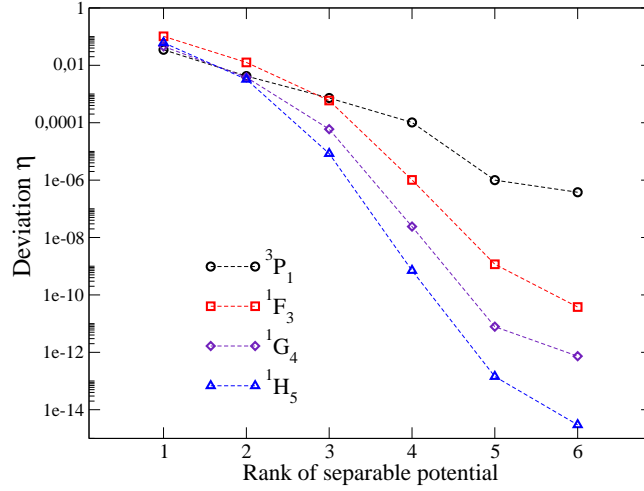


FIG. 4: (Color online) Squared deviation of the separable  $V_{\text{low-k}}^{[n]}(k, k')$  from the original  $V_{\text{low-k}}(k, k')$  for various uncoupled channels at  $\Lambda = 2 \text{ fm}^{-1}$ .

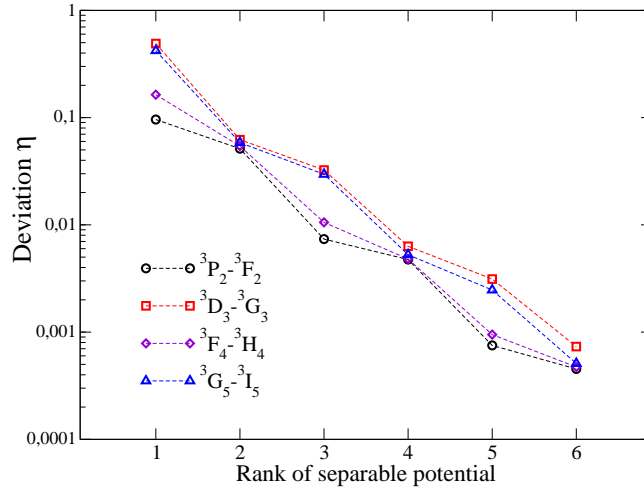


FIG. 5: (Color online) Squared deviation of the separable  $V_{\text{low-k}}^{[n]}(k, k')$  from the original  $V_{\text{low-k}}(k, k')$  for various coupled channels at  $\Lambda = 2 \text{ fm}^{-1}$ .

e.g., by means of the BHF approximation [28]. Recent relativistic calculations by van Dalen and M  ther demonstrate that saturation can be achieved within the  $V_{\text{low-k}}$  approach by inclusion of relativistic effects in dressing the Dirac spinors which are used to evaluate the underlying realistic interaction [35].

All the results obtained so far indicate that  $V_{\text{low-k}}^{[2,3]}$  is an accurate low-rank separable representation of  $V_{\text{low-k}}$  interaction. However, in order to make it accessible to other users, it should be parameterized in a simple form. Here we suggest the fitting function for all  $f_i(k)$  in all channels

$$f_i(k) = \alpha_i + (\beta_i \exp(\gamma_i k^{\delta_i}) + \mu_i) \sin(k\sigma_i + \lambda_i), \quad (12)$$

which contains 7 parameters for each partial wave channel and each  $f_i(k)$ . In the Table IV, we summarized all parameters of the separable fitted form for uncoupled channels, while all parameters for the coupled channels are shown in the Table V. By using the values from both tables one can reproduce the fitted version of  $V_{\text{low-k}}^{[2,3]}$  for a given partial wave channel. In the following we will identify the respective separable fitted potential as  $V_{\text{fit}}^{[2,3]}$ .

In order to check the accuracy of our fit we perform HF calculations of nuclear matter employing  $V_{\text{fit}}^{[2,3]}$ . The respective binding energy as a function of the density of symmetric nuclear matter are displayed on Fig.6 by a dashed-dotted line. One observes that at up to saturation density  $\rho_0 \simeq 0.16 \text{ fm}^{-3}$  the fitted potential  $V_{\text{fit}}^{[2,3]}$  reproduces the

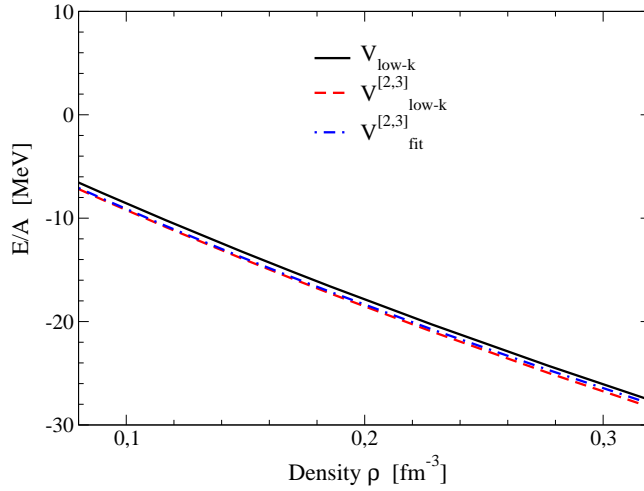


FIG. 6: (Color online) Energy per nucleon of symmetric nuclear matter as a function of the density. Results of  $V_{\text{low-k}}$  interaction (solid line) compared with the separable form  $V_{\text{low-k}}^{[2,3]}$  (dashed line) and the respective fitted form  $V_{\text{fit}}^{[2,3]}$  (dashed-dotted line).

Interaction	$t_0$ [MeV fm <sup>3</sup> ]	$t_3$ [MeV fm <sup>3+3α</sup> ]	$x_3$
CT	-584.1	8330.7	-0.5
CT1	-548.0	7890.13	-0.5
CT2	-565.467	8180.0	-0.5

TABLE I: Parameters of the contact interaction defined in Eq.(13). The set CT was produced for  $V_{\text{low-k}}$  [32], while CT1 and CT2 supply  $V_{\text{fit}}^{[2,3]}$ .

results of  $V_{\text{low-k}}^{[2,3]}$  (red dashed), while at higher densities it becomes slightly less bound and lies closer to the original  $V_{\text{low-k}}$  (solid). Thus the deviation of the fitted separable potential  $V_{\text{fit}}^{[2,3]}$  from  $V_{\text{low-k}}$  does not exceed 1% of binding energy. Not going into details we mention that the deviation rises mainly from  $^3S_1$ - $^3D_1$  and  $^3P_2$ - $^3F_2$  coupled channels.

As we have already seen from Fig.6  $V_{\text{low-k}}$  interaction as well as its separable form  $V_{\text{fit}}^{[2,3]}$  does not describe the empirical saturation point. In order to achieve the saturation in nuclear matter one has to add three-body interaction terms or a density-dependent two-nucleon interaction. Therefore we support the low-momentum interaction by a simple contact interaction, which have been chosen following the notation of the Skyrme interaction [15, 16]

$$\Delta\nu = \Delta\nu_0 + \Delta\nu_3, \quad (13)$$

with

$$\Delta\nu_0 = \frac{1}{4}t_0 [(2 + x_0)\rho^2 - (2x_0 + 1)(\rho_n^2 + \rho_p^2)] \quad (14)$$

and

$$\Delta\nu_3 = \frac{1}{24}t_3\rho^\alpha [(2 + x_3)\rho^2 - (2x_3 + 1)(\rho_n^2 + \rho_p^2)], \quad (15)$$

where  $\rho_p$  and  $\rho_n$  are the local densities of nucleons while the total matter density is denoted as  $\rho = \rho_p + \rho_n$ . The values of  $\alpha$  and  $x_0$  were fixed at  $\alpha = 0.5$ ,  $x_0 = 0.0$ , while  $t_0$ ,  $t_3$ ,  $x_3$  were fitted in such a way that HF calculations using  $V_{\text{low-k}}$  or  $V_{\text{fit}}^{[2,3]}$  plus the contact term (13) reproduces both the empirical saturation point of the symmetric nuclear matter and the symmetry energy at saturation density. Following [32] the contact interaction produced for  $V_{\text{low-k}}$  will be labeled by CT, and the respective interaction model  $V_{\text{low-k}} + \text{CT}$ . For the fitted potential  $V_{\text{fit}}^{[2,3]}$  we suggest two possible parameterizations: CT1 and CT2. Their parameters and properties of nuclear matter are shown in Tables I and II, respectively.



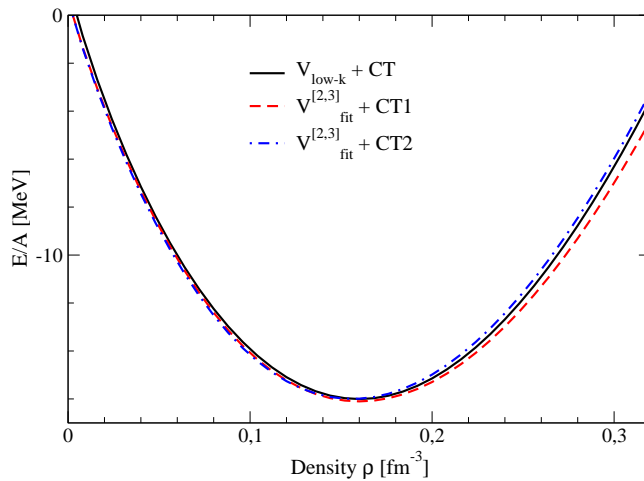


FIG. 7: (Color online) Energy per nucleon of symmetric nuclear matter as a function of the density. Results of  $V_{\text{low-k}} + \text{CT}$  interaction (solid line) compared with the fitted separable form  $V_{\text{fit}}^{[2,3]} + \text{CT1}$  (dashed line) and  $V_{\text{fit}}^{[2,3]} + \text{CT2}$  (dashed-dotted line).

Interaction	$\rho_0$ [fm $^{-3}$ ]	$E/A(\rho_0)$ [MeV]	$K$ [MeV]
$V_{\text{low-k}} + \text{CT}$	0.16	-16.0	258
$V_{\text{fit}}^{[2,3]} + \text{CT1}$	0.16	-16.1	241.9
$V_{\text{fit}}^{[2,3]} + \text{CT2}$	0.156	-16.0	240.5

TABLE II: Bulk properties of symmetric nuclear matter derived from  $V_{\text{low-k}}$  and its separable representation. They are supplemented by the respective contact interaction.

The interaction  $V_{\text{fit}}^{[2,3]} + \text{CT1}$  gives the binding energy per nucleon of symmetric nuclear matter  $E/A = -16.1$  MeV at the density  $\rho_0 = 0.16$  fm $^{-3}$ . The HF calculations of nuclear matter (see Fig.7) for  $V_{\text{fit}}^{[2,3]} + \text{CT1}$  give results (dashed line) very similar to the non-separable initial interaction  $V_{\text{low-k}} + \text{CT}$  (solid line). However, in calculation of finite nuclei we observe a deviation of about 0.12 MeV in the binding energy of light nuclei, like  $^{16}\text{O}$  (see Table III). The picture can be improved if we assume, that the saturation density is not defined exactly and allow for a small deviation. Along this line the second parameterization CT2 was produced. The interaction  $V_{\text{fit}}^{[2,3]} + \text{CT2}$  gives  $E/A = -16.0$  MeV at the density  $\rho_0 = 0.156$  fm $^{-3}$ . This corresponds to a small shift of the saturation point with respect to the initial  $V_{\text{low-k}}$  interaction (see Fig.7). It allows us to improve the accuracy in the binding energies of finite nuclei: one can notice that the contact interaction CT2 leads to a better description than CT1. However, comparing the rms charge radii of nuclei in Table III, we see that due to the shift in saturation density the interaction  $V_{\text{fit}}^{[2,3]} + \text{CT2}$  yields larger radii than the interaction  $V_{\text{fit}}^{[2,3]} + \text{CT1}$ .

For all models considered here the compressibility modulus at saturation density is in the range  $240.5 \leq K \leq 258$  MeV. This means that the respective equations of state displayed in Fig.7 are rather soft, at least at densities up to about two times saturation density. Such a prediction of a soft EoS is in agreement with data extracted from heavy ion reactions. For example, heavy ion data for transverse flow [36] or from kaon production [37] support the picture of a soft EoS in symmetric nuclear matter. This value for the compressibility modulus is also in agreement with that of the Skyrme interaction which reproduce correctly the breathing mode in nuclei (giant isoscalar resonance) [42].

#### IV. SUMMARY AND CONCLUSION

In the last decade it has become popular to perform nuclear structure calculations using the low-momentum NN interaction  $V_{\text{low-k}}$  (see for instance the recent Ref. [43, 44]). This interaction is constructed from a realistic NN interaction by introducing a cutoff  $\Lambda$  in the relative momenta of the interacting nucleons. We used a model space technique on the base of the unitary model operator approach to separate the low-momentum and high-momentum parts of the initial CD-Bonn interaction. The cutoff parameter  $\Lambda$  was fixed at  $\Lambda = 2$  fm $^{-1}$  so that a  $V_{\text{low-k}}$  is obtained,



Interaction	<sup>16</sup> O	<sup>40</sup> Ca	<sup>48</sup> Ca	<sup>60</sup> Ca	<sup>208</sup> Pb
	E/A [MeV]				
$V_{\text{low-k}} + \text{CT}$	-7.91	-8.57	-8.42	-7.75	-7.76
$V_{\text{fit}}^{[2,3]} + \text{CT1}$	-7.79	-8.56	-8.35	-8.78	-7.76
$V_{\text{fit}}^{[2,3]} + \text{CT2}$	-7.84	-8.58	-8.37	-8.79	-7.76
Experiment	-7.98	-8.55	-8.67	–	-7.87
	$r_{\text{ch}}$ [fm]				
$V_{\text{low-k}} + \text{CT}$	2.79	3.50	3.54	3.68	5.51
$V_{\text{fit}}^{[2,3]} + \text{CT1}$	2.81	3.51	3.55	3.68	5.52
$V_{\text{fit}}^{[2,3]} + \text{CT2}$	2.82	3.53	3.58	3.71	5.56
Experiment	2.74	3.48	3.47	–	5.50

TABLE III: The binding energy per nucleon and rms charge radii of finite nuclei. Experimental data taken from Refs. [38]-[41].

which is essentially independent on the underlying bare NN interaction.

The resulted  $V_{\text{low-k}}$  interaction is nonlocal and defined in terms of matrix elements in momentum space for each partial wave channel. This allows us to use a diagonalization method in order to express the matrix elements in a separable form. We investigate the separability in different channels with increase of the cutoff  $\Lambda$ . It was found that at  $\Lambda = 2 \text{ fm}^{-1}$  the low-momentum interaction can accurately be approximated by a low-rank separable interaction. This separable interaction is parameterized to make it accessible for other nuclear structure calculations.

A density dependent contact interaction is added to reproduce the saturation property of infinite nuclear matter. HF calculations using this interaction model also reproduce the bulk properties of finite nuclei with good accuracy. We demonstrate that this new separable representation of the  $V_{\text{low-k}}$  interaction, reproduces the results derived from the original  $V_{\text{low-k}}$  with a high accuracy.

This work has been supported by the European Graduate School “Hadrons in Vacuum, in Nuclei and Stars” (Basel, Graz, Tübingen) and a grant Mu 705/5-2 of the Deutsche Forschungsgemeinschaft (DFG) and by CompStar, a Research Networking Programme of the European Science Foundation.

Channel	$i$	$a_i$	$\alpha_i$	$\beta_i$	$\gamma_i$	$\delta_i$	$\mu_i$	$\sigma_i$	$\lambda_i$
$^1S_0$	1	-0.16344E+02	0.10772E-03	-0.43234E-03	0.17650E+00	0.92610E+00	0.10316E-02	0.99335E+00	0.14191E+01
	2	-0.66770E+00	-0.20749E-03	-0.18295E-01	0.66232E-01	0.86815E+00	0.20236E-01	0.17925E+01	0.11085E+01
$^1P_1$	1	0.14569E+02	-0.36052E-02	0.12380E-02	0.30093E+00	0.15720E+01	0.24098E-02	0.46996E+00	0.14196E+01
	2	0.15105E+01	0.41103E-04	-0.30056E-02	0.46402E-01	0.12591E+01	0.36618E-02	0.22676E+01	-0.66286E-02
$^3P_0$	1	0.36518E+01	0.34915E-04	-0.39191E-03	0.74648E-01	0.35155E+01	0.35779E-03	0.20292E+01	0.14199E+01
	2	-0.36339E+01	0.12254E-03	0.20982E-03	-0.59888E+00	0.10769E+01	0.30373E-03	-0.21878E+01	0.96652E+01
$^3P_1$	1	0.15410E+02	-0.33598E-03	0.15182E-02	-0.12701E-02	0.54199E+01	-0.85450E-03	0.59810E+00	0.52799E+00
	2	0.11011E+01	-0.44421E-03	0.18896E-02	-0.63158E+00	0.24471E+01	0.94546E-04	0.73498E+00	0.22558E+00
$^1D_2$	1	-0.47228E+01	0.23948E-03	0.11514E-02	0.78532E-01	0.83080E+00	-0.14043E-02	0.15502E+01	0.12639E+01
	2	-0.42720E+00	0.43276E-03	-0.13308E-02	-0.76108E+00	0.22797E+01	0.89215E-03	0.12810E+01	0.17046E+01
$^3D_2$	1	-0.14755E+02	0.23661E-03	-0.16214E-03	-0.20028E+00	0.47727E+01	-0.79636E-04	0.12915E+01	0.17118E+01
	2	-0.20625E+01	0.46873E-03	-0.13299E-02	-0.70797E+00	0.22075E+01	0.85842E-03	0.14395E+01	0.16497E+01
$^1F_3$	1	0.21276E+01	0.11682E-03	-0.24864E-03	-0.15328E+01	-0.76112E+00	-0.11725E-03	0.20029E+01	0.14366E+01
	2	0.45580E+00	0.45434E-03	0.34263E-02	-0.23846E+01	-0.12925E+01	-0.45576E-03	0.18623E+01	0.14425E+01
$^3F_3$	1	0.11895E+01	0.12811E-03	-0.89537E-04	-0.63186E+00	-0.13835E+01	-0.12893E-03	0.20960E+01	0.13909E+01
	2	0.26740E+00	0.44076E-03	0.35397E-02	-0.24171E+01	-0.12481E+01	-0.44204E-03	0.18298E+01	0.14500E+01
$^1G_4$	1	-0.56713E+00	0.93511E-04	-0.32673E-03	-0.14289E+01	-0.10215E+01	-0.94613E-04	0.19148E+01	0.13505E+01
	2	-0.09176E+00	0.92267E-02	-0.14963E-01	-0.55660E+01	-0.18735E+01	-0.92335E-02	-0.37857E+00	0.16284E+01
$^3G_4$	1	-0.30270E+01	0.10774E-03	-0.16121E-03	-0.77810E+00	-0.15648E+01	-0.10940E-03	0.18745E+01	0.13214E+01
	2	-0.5061E+00	0.10191E-03	-0.62066E-03	-0.10817E+01	-0.10648E+01	-0.10392E-03	0.31194E+01	0.13385E+01
$^1H_5$	1	0.06095E+01	0.14458E-06	-0.43467E-03	-0.30481E+00	0.34986E+01	0.43536E-03	0.13486E+01	-0.29605E+00
	2	0.01455E+01	0.99849E-04	-0.38155E-03	-0.64624E+00	-0.24138E+01	-0.10803E-03	0.33677E+01	0.95975E+00
$^3H_5$	1	0.03736E+01	0.17206E-06	-0.45636E-03	-0.28889E+00	0.34083E+01	0.45708E-03	0.13780E+01	-0.31990E+00
	2	0.00727E+00	0.86739E-04	-0.36173E-03	-0.88687E+00	0.29817E+01	0.45115E-03	0.32408E+01	-0.20198E+01
$^1I_6$	1	-0.01407E+01	0.18615E-04	-0.27820E-04	0.15265E+01	0.97282E+00	0.15276E-04	0.20513E+01	0.15767E+01
	2	-0.00281E+01	0.63551E+00	-0.26703E+00	0.18734E+00	0.19309E+01	-0.36758E+00	0.39862E+00	0.15760E+01
$^3I_6$	1	-0.08297E+01	-0.18713E-04	-0.30695E+00	0.31341E-03	0.21961E+01	0.30694E+00	0.19374E+01	0.16207E+01
	2	-0.0153E+01	0.94460E-04	-0.30640E+00	0.53129E-03	0.14854E+01	0.30630E+00	0.33132E+01	0.79134E+00

TABLE IV: Parameters of  $V_{\text{fit}}^{[2,3]}$  for uncoupled channels. See Eq.(12).

- [1] R. Machleidt, F. Sammarruca, and Y. Song, Phys. Rev. C **53**, R1483 (1996).
- [2] R. B. Wiringa, V. G. Stoks, and R. Schiavilla, Phys. Rev. C **51**, 38 (1995).
- [3] V. G. Stoks, R. A. M. Klomp, C. P. F. Terheggen, and J. J. de Swart, Phys. Rev. C **49**, 2950 (1994).
- [4] D. R. Entem and R. Machleidt, Phys. Rev. C **68**, 041001(R) (2003).

Channel	$i$	$\alpha_i$	$\alpha_i$	$\beta_i$	$\gamma_i$	$\delta_i$	$\mu_i$	$\sigma_i$	$\lambda_i$
$^3S_1$	1	-0.39195E+02	0.14710E-03	-0.27882E-02	0.10166E+00	0.98761E+00	0.33148E-02	0.73493E+00	0.91775E+00
	2	0.20913E+02	-0.97562E-04	0.33292E+00	0.50609E-03	0.87732E+00	-0.33339E+00	0.14274E+01	0.12444E+01
	3	-0.46417E+01	-0.21867E-04	0.31258E+00	0.17566E-02	0.78784E+00	-0.31368E+00	0.18855E+01	0.11761E+01
$^3D_1$	1	-0.39195E+02	0.90122E-04	0.31369E-05	0.38917E-03	0.12444E+02	-0.93123E-04	0.13384E+01	0.15561E+01
	2	0.20913E+02	0.11207E-03	-0.13705E-04	0.48296E+00	0.24592E+01	-0.97861E-04	0.21818E+01	0.15329E+01
	3	-0.46417E+01	-0.22645E-03	-0.41235E+00	0.40973E-03	0.18283E+01	0.41258E+00	0.15668E+01	0.15335E+01
$^3P_2$	1	-0.11712E+02	-0.12771E-01	0.74967E-02	0.29157E-01	0.83736E+00	0.53084E-02	0.11992E+00	0.14904E+01
	2	-0.21898E+01	-0.92101E-04	0.28219E+00	0.19554E-02	0.11980E+01	-0.28296E+00	0.12014E+01	-0.12709E+00
	3	0.17808E+01	0.14009E-03	0.34622E+00	0.13719E-02	0.12162E+01	-0.34694E+00	0.12159E+01	0.29393E+01
$^3F_2$	1	-0.11712E+02	-0.37975E-05	-0.26753E-09	0.11862E+02	0.11520E+00	-0.69054E-05	0.10568E+01	-0.53109E+00
	2	-0.21898E+01	0.71589E-04	-0.98497E-14	0.22438E+02	0.54423E-01	-0.69308E-04	-0.23032E+01	-0.46525E+01
	3	0.17808E+01	0.24733E-03	-0.69363E-04	0.12429E+01	0.45015E+00	0.40433E-03	0.11919E+01	0.40019E+01
$^3D_3$	1	-0.60466E+01	0.18332E-03	0.14266E+00	0.41443E-03	0.17445E+01	-0.14284E+00	0.21656E+01	0.15038E+01
	2	0.54641E+01	-0.27373E-03	-0.45681E+00	0.67993E-03	0.90916E+00	0.45713E+00	0.18906E+01	0.99510E+00
	3	0.91410E+00	-0.11606E-03	0.18114E+00	-0.13213E+00	0.12510E-02	-0.15901E+00	0.33728E+01	-0.79666E+00
$^3G_3$	1	-0.60466E+01	0.41921E-04	-0.65759E-01	0.79378E-03	0.18207E+01	0.65717E-01	0.14240E+01	0.16750E+01
	2	0.54641E+01	0.15808E-03	-0.16419E-03	-0.10345E+00	-0.99477E+00	0.28959E-03	0.19522E+01	-0.25907E+01
	3	0.91410E+00	0.78827E-04	-0.73989E-01	-0.17382E-02	0.15332E+01	0.74065E-01	0.30794E+01	-0.18745E+01
$^3F_4$	1	-0.16095E+01	0.18033E-03	0.37879E+00	-0.39428E-03	0.37390E+00	-0.37852E+00	0.21928E+01	-0.23390E+01
	2	0.56160E+00	0.24168E-03	-0.11138E+01	-0.80823E-04	0.27458E+01	0.11135E+01	0.19919E+01	0.13089E+01
	3	-0.30360E+00	-0.32058E-03	-0.11873E+01	0.28972E-03	0.16371E+01	0.11877E+01	0.20173E+01	0.11166E+01
$^3H_4$	1	-0.16095E+01	0.30449E-07	0.28581E-01	-0.69621E+01	-0.54467E+00	0.15057E-05	0.10041E+01	0.30546E+01
	2	0.56160E+00	0.17531E-04	0.22351E+00	0.34114E-03	0.19278E+01	-0.22349E+00	0.16346E+01	-0.12499E+01
	3	-0.30360E+00	-0.14910E-02	0.20920E+00	0.26023E-02	0.24400E+01	-0.20770E+00	0.59266E+00	0.16380E+01
$^3G_5$	1	0.16137E+01	-0.93523E-04	-0.48952E+00	-0.88510E-04	0.10928E+01	0.48961E+00	0.25801E+01	0.11545E+01
	2	-0.12501E+01	0.13111E-03	-0.13521E+00	-0.10757E+00	0.10162E-02	0.12130E+00	0.28269E+01	0.70560E+00
	3	0.30880E+00	-0.31841E-03	-0.53598E+00	0.61243E-03	0.18397E+01	0.53633E+00	0.23654E+01	0.99154E+00
$^3I_5$	1	0.16137E+01	0.14023E-04	0.36754E+00	-0.14039E-03	0.25880E+01	-0.36755E+00	0.17978E+01	0.15991E+01
	2	-0.12501E+01	0.19169E-04	0.29512E+00	0.15469E-03	0.26251E+01	-0.29510E+00	0.17038E+01	-0.16316E+01
	3	0.30880E+00	0.38821E-04	0.36156E+00	0.35017E-03	0.19665E+01	-0.36153E+00	0.30449E+01	-0.21756E+01
$^3H_6$	1	-0.30540E+00	-0.65438E-03	0.65143E+00	0.56031E-03	0.23634E+01	-0.65075E+00	0.48747E+00	0.18318E+01
	2	0.20960E+00	0.61333E-04	0.25966E+00	-0.32893E-03	0.13102E+01	-0.25972E+00	0.25754E+01	0.11963E+01
	3	-0.63700E-01	0.25601E-03	0.39808E+00	0.29243E-03	0.32313E+01	-0.39836E+00	0.22583E+01	0.10325E+01
$^3K_6$	1	-0.30540E+00	-0.10269E-04	0.23504E+00	0.14785E-03	0.31131E+01	-0.23503E+00	0.18245E+01	0.14457E+01
	2	0.20960E+00	0.12093E-04	-0.36799E+00	0.11473E-03	0.30036E+01	0.36798E+00	0.18060E+01	0.14804E+01
	3	-0.63700E-01	-0.19663E-04	0.26322E+00	0.39336E-03	0.23907E+01	-0.26320E+00	0.29488E+01	0.91309E+00

TABLE V: Parameters of  $V_{\text{fit}}^{[2,3]}$  for coupled channels. See Eq.(12).

- [5] M. Baldo, in *Nuclear Methods and the Nuclear Equation of State*, edited by M. Baldo (World Scientific 1999).
- [6] E. Feenberg, in *Theory of Quantum Fluids*, (Academic Press 1969).
- [7] R. B. Wiringa, S. C. Pieper, J. Carlson and V. R. Pandharipande, Phys. Rev. C **62**, 044310 (2000).
- [8] W. H. Dickhoff and D. Van Neck, *Many-Body Theory Exposed!* (World Scientific, Singapore, 2005).
- [9] P. Gögelein, E. N. E. van Dalen, Kh. Gad, Kh. S. A. Hassaneen, and H. Mütter, Phys. Rev. C **79**, 024308 (2009).
- [10] A. Fabrocini, S. Fantoni, A. Yu. Illarionov, K. E. Schmidt, Nucl. Phys. **A803**, 137 (2008).
- [11] N. Farina, PhD Thesis, Universita di Roma, 2008.
- [12] O. Benhar, A. Carbonne, arXiv:nucl-th/0912.0129 (2009).
- [13] M. Baldo, U. Lombardo, É. E. Saperstein, and S. V. Tolokonnikov, JETP letters **80**, 523 (2004).
- [14] M. Baldo, P. Schuck, X. Viñas, Phys. Lett. **B663**, 390 (2008).
- [15] T. H. R. Skyrme, Nucl. Phys. **9**, 615 (1959).
- [16] D. Vautherin and D. M. Brink, Phys. Rev. C **5**, 626 (1972).
- [17] J. W. Negele and D. Vautherin, Nucl. Phys. **A207**, 298 (1973).
- [18] J. Margueron, J. Navarro, and N. Van Giai, Phys. Rev. C **66**, 014303 (2002).
- [19] J. Margueron and H. Sagawa, J. Phys. G: Nucl. Part. Phys. **36**, 125102 (2009).
- [20] S. K. Bogner, T. T. S. Kuo, and L. Coraggio, Nucl. Phys. **A684**, 432c (2001).
- [21] S. Y. Lee and K. Suzuki, Phys. Lett. **B91** 173 (1980).
- [22] S. Okubo, Prog. Theor. Phys. **12**, 603 (1954).
- [23] S. K. Bogner, R. J. Furnstahl, and A. Schwenk, arXiv:nucl-th/0806.1365 (2008).
- [24] K. Suzuki, Prog. Theor. Phys. **68**, 246 (1982).
- [25] M. Baldo and L. S. Ferreira, Nucl. Phys. **A480**, 271 (1988).
- [26] Y. Tian, Z.-Y. Ma, and P. Ring, Phys. Rev. C **80**, 024313 (2009).
- [27] H. Kamada *et al.*, Prog. Theor. Phys. **115**, 839 (2006).
- [28] P. Božek, D.J. Dean, and H. Mütter, Phys. Rev. C **74**, 014303 (2006).
- [29] S. Fujii, R. Okamoto, and K. Suzuki, Phys. Rev. C **69**, 034328 (2004).
- [30] J. Kuckei, F. Montani, H. Mütter, and A. Sedrakian, Nucl. Phys. **A723**, 32 (2003).
- [31] F. Montani, C. May, and H. Mütter, Phys. Rev. C **69**, 065801 (2004).
- [32] E. N. E. van Dalen, P. Gögelein and H. Mütter, Phys. Rev. C **80**, 044312 (2009).
- [33] J. Haidenbauer and W. Plessas, Phys. Rev. C **30**, 1822 (1984).
- [34] S. K. Bogner, A. Schwenk, R. J. Furnstahl, and A. Nogga, Nucl. Phys. **A763**, 59 (2005).
- [35] E. N. E. van Dalen and H. Mütter, Phys. Rev. C **80**, 037303 (2009).
- [36] G. Stoicea *et al.* (FOPI Collaboration), Phys. Rev. Lett. **92**, 072303 (2004).
- [37] C. Sturm *et al.* (KaoS Collaboration), Phys. Rev. Lett. **86**, 39 (2001); C. Fuchs, A. Faessler, E. Zabrodin, Y. M. Zheng, *ibid.* **86**, 1974 (2001); C. Fuchs, Prog. Part. Nucl. Phys. **56**, 1 (2006).
- [38] B. A. Brown, Phys. Rev. C **58**, 220 (1998).

- [39] G. Audi, A. H. Wapstra, Nucl. Phys. **A565**, 1 (1993).
- [40] M. Chartier *et al.*, Phys. Rev. Lett. **77**, 2400 (1996).
- [41] G. Fricke *et al.*, At. Data. Nucl. Data Tables **60**, 177 (1995).
- [42] S. Shlomo, V. M. Kolomietz, G. Colò, Eur. Phys. J. A **30**, 23 (2006).
- [43] T. Lesinski, T. Duguet, K. Bennaceur, and J. Meyer, Eur. Phys. J. **A** 40, 121 (2009).
- [44] K. Hebeler, T. Duguet, T. Lesinski, and A. Schwenk, Phys. Rev. C **80**, 044321 (2009).